Journal of Magnetism and Magnetic Materials 353 (2014) 105–109

Contents lists available at ScienceDirect

Journal of Magnetism and Magnetic Materials

journal homepage: www.elsevier.com/locate/jmmm

Comparative study of the thermal fluctuations effects on the classical Stoner–Wohlfarth and analytical vector hysteron models

E. De Biasi*, C.A. Ramos, R.D. Zysler

Laboratorio de Resonancias Magnéticas, Centro Atómico Bariloche, CP 8400 S.C. de Bariloche, RN, Argentina

ARTICLE INFO

Article history:
Received 18 September 2013
Received in revised form
21 October 2013
Available online 29 October 2013

Keywords:
Stoner–Wohlfarth model
Analytical vector hysteron model
Hysteretic behavior model
Magnetization inversion

ABSTRACT

In this work we present a comparative study of the classical Stoner Wohlfarth model and the analytical vector hysteron model. We analyze the hysteretic behavior description when the thermal fluctuations are included. We found a different behavior in the evolution of the coercive field as function of temperature for the vector hysteron model when the anisotropy easy axis is non-parallel to the magnetic field orientation. At low temperatures a plateau is observed as consequence of the switching field behavior. At high temperature both models give identical description of the magnetization behavior, which merges with the superparamagnetic approximation.

1. Introduction

The magnetic characterization of nanoparticles is an issue that has taken the attention of the scientist in the last years. It is well known the wide range of application in magnetic recording [1], drug delivery [2], as contrast agent in tomography studies [3], hyperthermia [4], spintronic [5], etc. In each of these cases, certain features on the magnetic behavior are required with the purpose of facilitating their application. In order to tune the magnetic properties it becomes essential to have a model that describes the magnetization characteristics, as magnetic relaxation, the interactions effects, frustration, etc. In this sense the Stoner–Wohlfarth model (SW) [6] gives an accurate description that fits very well for non-interacting single domain nanoparticle systems. Although this model provides a description at zero temperature, it is possible to include thermal effects through stochastic calculations (Fokker–Planck equation [7], Monte Carlo [8,9]) or simply considering the magnetization passage over the energy barrier (Néel–Brown model [10,11]). However, the SW model has some inaccuracies in the hysteresis loop description as the external magnetic field is applied close to the perpendicular easy axis orientation, giving a behavior that is known as the magnetization "crossover" [12]. In addition, it is well known that the SW model can be solved analytically only in the parallel and perpendicular configurations; in all the other cases a numerical approach is necessary. There have been several modifications and approximations in the theory of SW to improve the description of the experimental data with these theories [11,12] that include the evolution with temperature and with magnetic field, thus achieving accurate superparamagnetic-blocked regime crossover, the $M(H)$ curves (irreversibility and coercive fields, etc.) [14]. Petrila and coworkers have presented an interesting proposal to describe the ferromagnetic single domain nanoparticle behavior [13,14]. This model, called analytical vector hysteron (VH), "keeping the macrospin concept and by relaxing the symmetry conditions of the ferromagnetic particles" [15] propose to modify the expression of the uniaxial magnetic anisotropy replacing the $(\cos\theta)^2$ by $|\cos\theta|$. This linearization introduces some mathematical advantages, because the treatment of the problem becomes completely analytical, at difference with the SW model, and also the model provides a solution to the crossover problem.

However, we found that both models do not describe satisfactorily the magnetic hysteresis loops at low temperatures, giving a plateau in the thermal coercive field evolution. In view of this, it seems important to contrast the predicted behaviors (assuming the hypotheses are fulfilled) with the experimental evidence.

2. SW and VH models: basic assumptions

In this section we present the hypothesis associated to both models, which have many common characteristics. First, both models describe the energy angular dependence assuming that

a) the particles are single domain uniformly magnetized.
b) The particles are monodipersed (this does not represent a fundamental restriction, and it can be avoided in a later treatment, simply integrating the magnetization weighed by a size distribution).

* Corresponding author. Tel.: +54 294 4445158.
E-mail address: debiasi@cab.cnea.gov.ar (E. De Biasi).

0304-8853/$ - see front matter © 2013 Elsevier B.V. All rights reserved.
http://dx.doi.org/10.1016/j.jmmm.2013.10.031

c) The coherent magnetization inversion is assumed.
d) The particles are non-interacting (or the effects of the interactions can be treated as an effective uniaxial anisotropy).
e) The particles have an effective uniaxial anisotropy (from several sources: magnetostatic, magnetocrystalline, interactions, etc.).
f) The effective anisotropy and the magnetization remain unaltered with temperature.
g) The “experimental time window” is larger than the intrinsic relaxation time (associated to the inverse of the damping parameter in the Landau–Lifshitz–Gilbert equation). Then, the orientation of the magnetic moment is along the local energy minimum.
h) In this description we neglect the oscillations of the magnetization around the local energy minimum due to thermal fluctuations.
i) The Master Equation gives the thermal evolution of the magnetic population of the energy minima.
j) The particles remain at rest, that is, without changing position or rotating. Then the relaxation mechanism is the Néel-Brown to overcome the energy barrier.
k) We assume valid the Arrhenius law for the effective passage time of the magnetization orientation from a minimum to the other.

The energy expression consists of two terms: the Zeeman one, which describes the effects of an external magnetic applied field (identical in both models), and the anisotropy term. In Eq. (1) we introduce the energy expressions E_{SW} and E_{VH} corresponding to SW and VH models respectively:

$$E_{SW} = -\vec{u}\cdot\vec{H} - K_{SW}V(\hat{n}\cdot\hat{u})^2$$
$$E_{VH} = -\vec{u}\cdot\vec{H} - K_{VH}V|\hat{n}\cdot\hat{u}| \quad (1)$$

In these expressions $\vec{u}$ is the magnetization vector, $\vec{H}$ the external magnetic field, V the particle volume, $\vec{n}$ ($\vec{u}$) is the unitary vector along the easy axis (magnetization) orientation, and $K_{SW} \cong 8/3\,\pi\,K_{VH}$ are the anisotropy constants. In both cases the energy remains unaltered under inversion ($\vec{n} \leftrightarrow -\vec{n}$). Eq. (1) shows that the difference between the SW and the VH models is given by the anisotropy term definition. The SW description provides a continuously differentiable energy expression at difference with the VH model. On the other hand, the VH model allows obtaining analytical expressions for the magnetization, energy barrier, coercive (H_C) and switching (H_S) fields, which makes this model easy to apply, saving computation time. Conversely, in the SW model only H_C and H_S have a closed expression for any applied field orientation; the magnetization, for instance, must be calculated finding numerically the equilibrium orientation of $\vec{\mu}$ for each $\vec{H}$. The analytical expression for the ($\pm$) branches of a normalized hysteresis loop in the VH model is given by

$$m_{\pm} = \frac{\mu H \pm KV\cos(\psi)}{\sqrt{K^2V^2 + \mu^2H^2 \pm 2KV\mu H\cos(\psi)}} \quad (2)$$

where ψ is the angle between the field and easy axis orientation and $K = K_{VH}$. Eq. (2) must be used according with the switching condition given in Eq. (18) of [15].

In the SW model the switching field, H_S has a closed expression, which can be compared with the VH one:

$$H_{S\_SW} = H_{0\_SW}\left[\sin^{2/3}(\psi) + \cos^{2/3}(\psi)\right]^{-\frac{3}{2}}$$
$$H_{S\_VH} = H_{0\_VH}/[2\cos(\psi)] \quad (3)$$

where $H_{0\_SW} = 2K_{SW}V/\mu$ and $H_{0\_VH} = 2K_{VH}V/\mu$.

In the SW model when H is increased the maxima and minima change their orientation gradually and only one minimum remains for $H \geq H_{S\_SW}$. In the VH model only the minima changes their equilibrium orientation (given the magnetization expression of Eq. 2), the maxima remains always perpendicular to $\hat{n}$. Also, when we approach the perpendicular configuration ($\hat{n} \perp \vec{H}$) H_{S_VH} field diverges, as shown by Eq. (3). This divergent behavior is clearly different from the results of the SW model. It has been interpreted within the context of some effective interparticle interaction [15] (exchange, for example). In fact, in a multidomain system it is necessary to consider energy terms such as: exchange, surface anisotropy, and magnetostatic energy. If they can be approximated as an effective uniaxial anisotropy, the treatment can be regarded as a single entity. However, it is difficult to justify this H_{S_VH} divergent behavior in a non-interacting nanoparticle system.

In the same way, the coercive field for both models can be compared:

$$H_{C\_SW} = H_0\begin{cases}\left[\sin^{2/3}(\psi) + \cos^{2/3}(\psi)\right]^{-\frac{3}{2}} \\ \sin(2\psi)/2\end{cases} \quad (4)$$

$$H_{C\_VH} = H_0\,\cos(\psi)/2$$

Eq. (1)–(4) corresponding to the VH model are quoted from references [15] and [16].

In the SW model, the coercive field needs to be considered in two different cases. In the first case, when $\psi < \pi/4$, the passage of the magnetization from a minimum to other occurs when the energy barrier disappears and the system remains with only one energy minimum. For this reason, the coercive field H_{C_SW} and the irreversibility field H_{S_SW} have the same expression. We refer to the energy barrier reduction towards a single energy minimum as a first “mechanism”. In the second case, for $\psi > \pi/4$, the magnetization vanishes by orienting the metastable energy minimum perpendicular to the magnetic field H, so that its projection is zero, but the system continues to have two energy minima. We call this a second “mechanism”. These two “mechanisms” manifest in very different ways. In the first case there is a sudden jump of the magnetization, while in the second case, the magnetization vanishes and changes sign continuously. Moreover, in the first case both branches of the hysteresis loop collapse, while in the second case it is possible to continue observing irreversibility, indicating that $H_{S\_SW} > H_{C\_SW}$. Unlike this, in the VH model, only the second mechanism is observed (except in the case $\psi = 0$, the only value for which $H_{S\_VH} = H_{C\_VH}$). In Fig. 1 hysteresis loops are shown for the SW (upper panel) and VH models (lower panel). Each panel shows two hysteresis loops illustrating the cases stated above.

2.1. H_C thermal evolution

One of the most important aspects expected for a magnetic monodomain model is to be able to describe the thermal evolution of the system. In monodispersed size systems is well known that the behavior is characterized by a decrease of the coercive field monotonically with temperature. The main effect of temperature on a hysteresis loop is to assist the magnetization reversal by reducing the value of the switching field. This topic presents one of the fundamental problems of the VH model because, as we have seen in the Eq. (3), H_{S_VH} diverges when ψ approaches $\pi/2$. Petrila and co-workers have studied the thermal evolution of the coercive field [16] comparing VH and SW models. However, their study is restricted to the case $\vec{H} \parallel \hat{n}$, that is $\psi = 0$. In order to consider other configurations, we study this problem including the thermal effects using the Master Equation [13] in order to calculate the temporal evolution of the minima population. We assumed that the characteristic relaxation time follows the Arrhenius law: $\tau = \tau_0 e^{-\Delta E\,\beta}$, where ΔE is the energy anisotropy barrier, β is the inverse of the thermal energy value, and τ_0 is the relaxation time in the limit $\beta \to 0$.

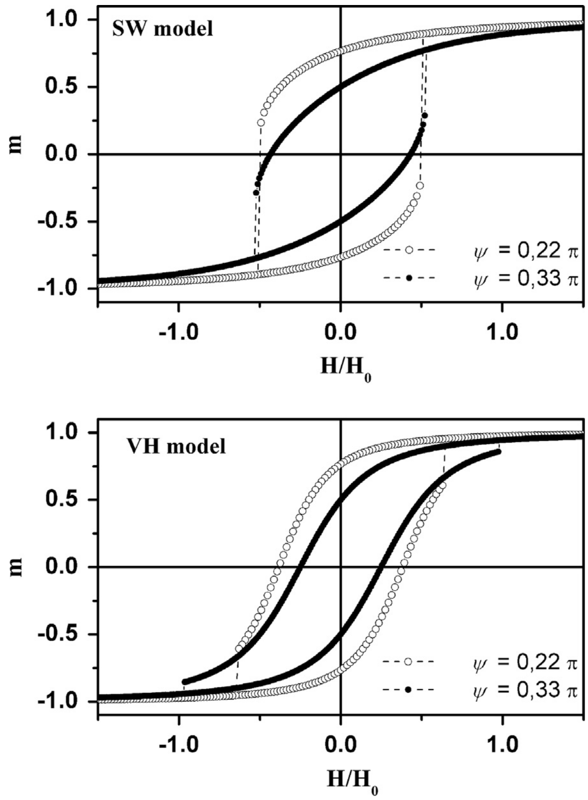

Fig. 1. Hysteresis loops simulations corresponding to the SW (top) and VH (bottom) models. Note the behavior of the magnetization when H achieves the coercive field value.

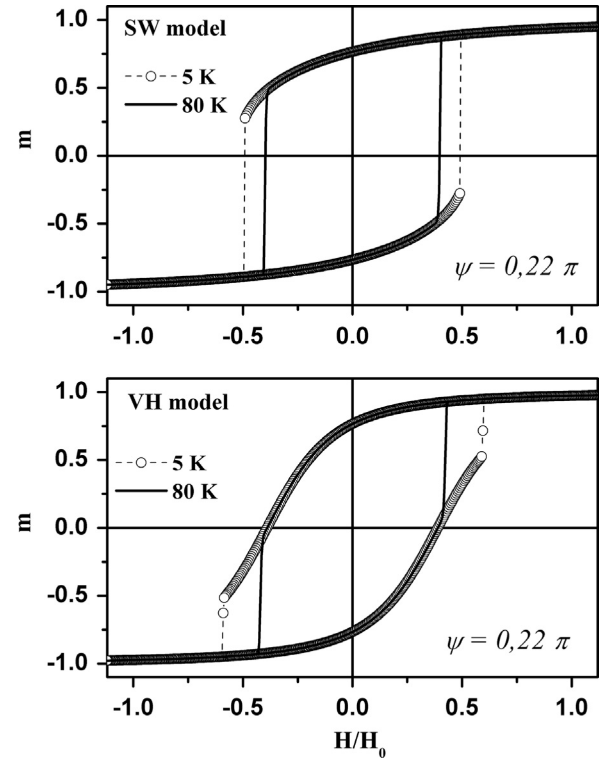

Fig. 2. Hysteresis loops simulations corresponding to the SW (top) and VH (bottom) models for T=5 K and T=80 K ($\psi < \pi/4$).

In Fig. 2 we show simulated hysteresis loops corresponding to SW (top) and VH (bottom) models for $\psi = 0.22\,\pi$. The calculations are made assuming the ratio between τ_0 and the measuring time is $\tau_0/\tau_m = 5 \times 10^{-12}$ (typical of a vibrating sample magnetometer). In both cases T=5 K and T=80 K loops are simulated in order to show the thermal effects in each model. In the SW case we can observe the change in H_{C_SW} as a consequence of the diminution of H_{S_SW}. However, in the VH case the H_{S_VH} reduction has not effect on H_{C_VH}, which remains constant.

In the top of Fig. 3 the thermal evolution of H_{C_VH} and H_{C_SW} for this particular configuration ($\psi = 0.22\,\pi$) are presented. The horizontal dash line indicates the zero temperature H_{C_VH} value, according Eq. (4). In the bottom of Fig. 3 we show the thermal evolution of H_C for both models for a particular case $\psi > \pi/4$ ($\psi = 0.33\,\pi$). As it can be seen in this case, both models have the same problem (a plateau on the H_C behavior), being it more significant in the VH case, which starts at higher temperature than the SW case (260 K and 40 K respectively).

The reason for the plateau in the H_C thermal evolution is the same for both models. Due to the hypothesis used in this work, we associate the decrease of H_S only to thermal fluctuations which facilitate the overcoming of the magnetic energy barrier. So, when $H_S > H_C$, it appears the mentioned problem at low temperatures. For the VH model this happens for $\psi > 0$ and, in the SW model, for $\psi > \pi/4$ (for $\psi \le \pi/4 H_{C\_SW} = H_{S\_SW}$). In both cases H_C represent the field for which the magnetization is oriented perpendicular to the direction of the applied magnetic field, and then its projection over the field direction is null. When $\psi \le \pi/4$ in the SW model the plateau is not observed.

In order to compare the models with conditions more commonly found in experiments, Fig. 4 shows the thermal evolution of H_C for randomly oriented easy axes. While H_{C_SW} evolves decreasing monotonically with temperature, H_{C_VH} shows an unexpected

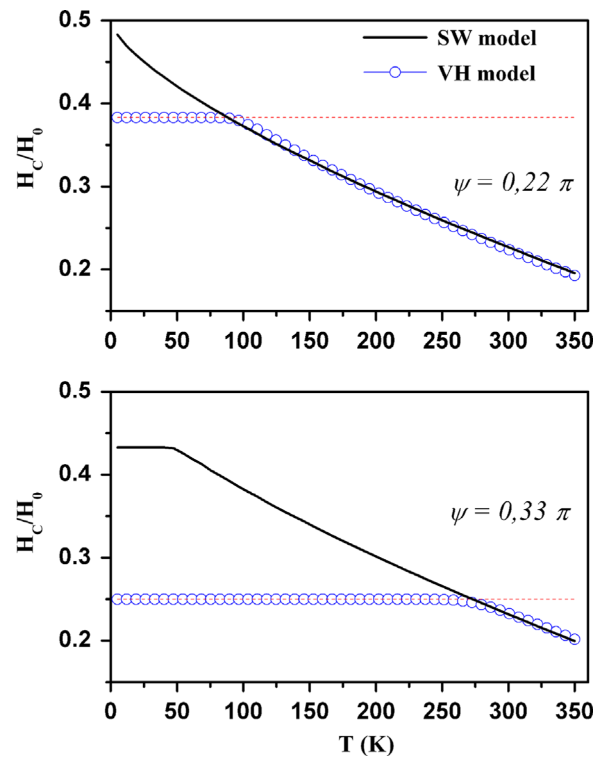

Fig. 3. Thermal evolution of the coercive field calculated for both models. The top panel corresponds to $\psi < \pi/4$ case and the bottom one to $\psi > \pi/4$.

behavior below 170 K. These results indicate that both SW and VH models are not suitable, in term of the present analysis, to describe the expected thermal behavior of an ideal randomly-oriented single-domain nanoparticle system.

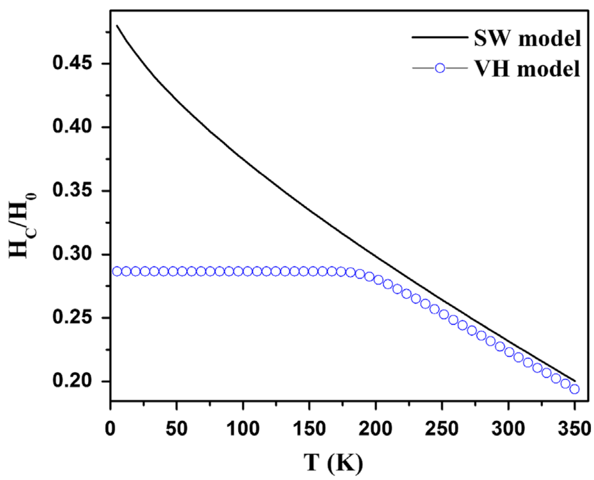

Fig. 4. Thermal evolution of the coercive field corresponding to a random easy axis.

2.2. High temperature regime

A useful limit to validate a model is the high temperature approximation. Then, we have studied the high temperature behavior of the VH model in order to compare it with the SW behavior. It is well-known that in the high temperature regime, i.e., when the thermal energy dominates, the magnetic system is in thermal equilibrium. Of course we are assuming that the experimental time window is larger than the relaxation time of the particle. In this case, the effective anisotropy diminishes and, particularly in presence of randomly oriented particles, the magnetization can be described by the Langevin function. In order to consider the thermal fluctuations on the magnetization behavior we applied the well-known expression:

$$m = \frac{1}{\beta}\frac{\partial \ln(Z)}{\partial H} \tag{5}$$

where the partition function is given by: $Z = \int e^{-E(\theta,\varphi)\beta}\, d\Omega$, and the integration is over all the states in the (θ,φ) plane. Making a Taylor series expansion for $\beta \to 0$, it can be obtained the high temperature approximation. The corresponding expression for SW and VH models are:

$$\begin{aligned} m_{SW} &\approx \frac{\mu H}{3}\beta + \frac{\mu HKV(1+3\ \cos(2\ \psi))}{45}\beta^2 + \frac{\mu H\left[2(K\ V)^2 - 21(H\mu)^2 + 6\ (KV)^2\ \cos(2\psi)\right]}{945}\beta^3 \\ m_{VH} &\approx \frac{\mu H}{3}\beta + \frac{\mu HKV(1+3\ \cos(2\ \psi))}{48}\beta^2 + \frac{\mu H\left[(K\ V)^2 - 32(H\mu)^2 + 3\ (KV)^2\ \cos(2\psi)\right]}{1440}\beta^3 \end{aligned} \tag{6}$$

Eq. (6) shows that, in the high temperature limit, the magnetization expressions for both models are very similar. The first term in β gives the Curie behavior predicted by the Langevin function. Small differences are found in the β^2 and β^3 terms. In order to compare with a more realistic system of nanoparticles, we can assume a random easy axis orientation and perform an integration over ψ, obtaining

$$m_{SW} = m_{VH} \approx \frac{\mu H}{3}\beta - \frac{(\mu H)^3}{45}\beta^3 \tag{7}$$

We observe that both expression merges exactly to the Taylor series expansion of the Langevin function.

Both models attempt to reproduce, under some limitations, the behavior of the magnetization of nanoparticle systems. The SW model describes accurately non-interacting nanoparticle systems, while VH describes system of particles with effective uniaxial anisotropy.

Models SW and VH can be used like a starting point for more realist treatments, that may relax some of the conditions imposed in their hypotheses to describe better the experimental evidences. In this sense, one can consider the effect of thermal fluctuations on the magnetization, the effective anisotropy [17–20], size and anisotropy distributions [21], other anisotropy symmetries [22], weak and moderate dipolar interactions [23], exchange between grains [24], etc.

To do an adequate treatment it is important to consider the characteristics and fundamental limitations of the starting model (SW or VH) together with the particularities of each system.

3. Conclusion

We have made a comparative study of the Stoner–Wohlfarth and the analytical Vector Hysteron models and theirs predictions for a randomly oriented nanoparticle system. Accordingly, we conclude that both models can be used satisfactorily to reproduce the hysteresis behavior of uniaxial identical single domain nanoparticle system with some limitation due to the approximations assumed. In the SW model the functional dependence of the uniaxial anisotropy energy induces the appearance of the crossover close to the perpendicular orientation of the easy axis with respect to the applied field ($\psi \approx \pi/2$), which is not observed in the VH model. In addition, the SW can be solved analytically only for $\psi = 0$ and $\psi = \pi/2$ cases. Contrarily, the VH model has analytic solutions for any value of ψ. In counterpart, it is necessary to be careful when the switching field is analyzed, because the VH shows a divergent behavior (at $\psi = \pi/2$) that cannot be associated to a single domain nanoparticle and it may be interpreted as the consequence of an effective exchange anisotropy. On the other hand, both models exhibit some difficulties when describing the thermal evolution of H_c.

Assuming the temperature is high enough so that the system has achieved thermal equilibrium the SW and VH models give an almost identical description of the magnetization behavior, which in addition, is consistent with the high temperature Langevin function approximation.

Acknowledgments

The authors thank to Universidad Nacional de Cuyo, Conicet, and ANPCYT (Argentina) grants.

References

[1] G.C. Hadjipanayis, Magnetic Storage Systems Beyond, Kluwer Academic, Dordrecht, 2000;
V. Skumryev, S. Stoyanov, Y. Zhang, G. Hadjipanayis, D. Givord, J. Nogués, Nature 423 (2003) 850.
[2] H.Wim De Jong, J.A.Paul Borm, Int. J. Nanomed. 3 (2008) 133.
[3] Shashi K Murthy, Int. J. Nanomed. 2 (2007) 129.
[4] B. Thiesen, A. Jordan, Int. J. Hyperth. 24 (2008) 467.
[5] A.E. Berkowitz, K. Takano, J. Magn. Magn. Mater 200 (1999) 552.
[6] E.C. Stoner, E.P. Wohlfarth, Philos. Trans. R. Soc. A 240 (1948) 599.
[7] P. Jönsson, T. Jonsson, J.L. García-Palacios, P. Svedlindh, J. Magn. Magn. Mater. 222 (2000) 219.
[8] E. De Biasi, C.A. Ramos, R.D. Zysler, H. Romero, Phys. Rev. B. 65 (2002) 144416.
[9] E. De Biasi, R.D. Zysler, C.A. Ramos, H. Romero, D. Fiorani, Phys. Rev. B. 71 (2005) 104408.
[10] L. Néel, Ann. Geophys. 5 (1949) 99.
[11] W.F. Brown, Phys. Rev. 130 (1963) 1677.
[12] A. Stancu, IEEE Trans. Magn. 33 (1997) 2573.
[13] E. De Biasi, R.D. Zysler, C.A. Ramos, M. Knobel, J. Magn. Magn. Mater. 320 (2004) e312.
[14] V. Franco, A. Conde, J. Magn. Magn. Mater. 278 (2004) 28.
[15] I. Petrila, A. Stancu, J. Phys. Condens. Matter 23 (2011) 076002.
[16] I. Petrila, I. Bodale, C. Rotarescu, A. Stancu, Phys. Lett. A 375 (2011) 3478.
[17] R.S. de Biasi, T.C. Devezas, J. Appl. Phys. 49 (1978) 2466.

[18] Y.L. Raikher, V.I. Stepanov, Sov. Phys. J. Exp. Theor. Phys. 75 (1992) 764.
[19] E. De Biasi, R.D. Zysler, C.A. Ramos, M. Knobel, J. Magn. Magn. Mater. 320 (2008) e312.
[20] E. De Biasi, C.A. Ramos, R.D. Zysler, J. Magn. Magn. Mater. 262 (2008) 235.
[21] M.F. de Campos, F.A. Sampaio da Silva, E.A. Perigo, J.A. de Castro, J. Magn. Magn. Mater. 345 (2013) 147.
[22] A. Hillion, A. Tamion, F. Tournus, O. Gaier, E. Bonet, C. Albin, V. Dupuis, Phys. Rev. B 88 (2013)094419 88 (2013).
[23] E. Lima, E. De Biasi, M.V. Mansilla, M.E. Saleta, M. Granada, H.E. Troiani, F.B. Effenberger, L.M. Rossi, H.R. Rechenberg, R.D. Zysler, J. Phys. D: Appl. Phys. 46 (2013) 045002.
[24] I. Petrila, A. Stancu, J. Appl. Phys 109 (2011) 083937.